NMR study of hydrogen in ferromagnetic β-UH_3

Y. B. Barash and J. Barak
Soreq Nuclear Research Centre, Yavne 70600, Israel

M. H. Mintz
Nuclear Research Centre, Negev, P.O. Box 9001, Beer-Sheva 84190, Israel

(Received 3 June 1983; revised manuscript received 6 December 1983)

NMR of protons in ferromagnetic β-UH_3 was observed at 4.2 and 85 K in zero external magnetic field. The line was centered at $\nu_0=19.4$ MHz ($T=85$ K). This frequency yields a value of $n_f=(1.45\pm0.1)\mu_B$ for the uranium-ion magnetic moment. The large linewidth ($\Delta\nu\simeq6$ MHz) could be explained by a distribution of the dipolar fields at the proton sites. The spectrum was also measured in an external field. The line shape agrees well with measurements made previously for paramagnetic β-UH_3. Line broadening in an external field is due to distribution of demagnetization fields. The spin-spin relaxation time $T_2=90$ μsec (at 4.2 K) is well explained by the proton-proton dipolar interaction. T_2 becomes shorter at 85 K and is field dependent.

I. INTRODUCTION

The magnetic properties of UH_3 in its two allotropic forms α-UH_3 and β-UH_3 have been the subject of many studies since the discovery of the ferromagnetic order of this material below $T_C\simeq173$ K.[1] This high transition temperature makes UH_3 especially interesting in view of the absence of magnetic order in uranium metal. Several groups have measured the magnetization of β-UH_3 by different methods.[1-7] The measured values of the number of Bohr magnetons μ_B per uranium atom in the ferromagnetic n_f and paramagnetic n_p states, as well as the ferromagnetic T_C and paramagnetic Θ_C Curie temperatures, are given in Table I. A large spread in the magnetization, as found by different methods and in different samples, is seen in the table.

The uranium atom has the configuration of $[Rn]5f^36d7s^2$. The small radius of the $5f$ electrons would suggest that, as in the rare-earth atoms, the open shells of $5f$ electrons would give rise to local magnetic moments. The ground state of $5f^3$ is $^4I_{9/2}$ (such as that of Nd^{3+}), which has $n_f=3.27$ and $n_p=3.62$. The experimental values given in Table I show much smaller values for n_f and n_p. The full localization of these $5f$ electrons is thus in doubt. For the case of uranium metal, which is nonmagnetic, it was shown[8] that the radius of the $5f$ electrons is not quite as small when compared with the interatomic separation. Through the use of electronic band calculations it was found that the $5f$ electrons populate broad itinerant states which have strong hybridization with the very broad $6d$-$7s$ bands. This situation resembles the nonmagnetic transition metals more than the magnetic rare-earth metals. The electronic band structure of α-UH_3 and β-UH_3 was recently studied by Switendick.[9] By comparing the crystal structure of β-UH_3 (Fig. 1) with that of α-UH_3, he has shown similar distances of first uranium-uranium, uranium-hydrogen, and hydrogen-hydrogen neighbors in the two phases. The similar magnetic properties of uranium atoms in the two crystallographically inequivalent sites in β-UH_3,[5] indicate that the first-neighbor distances are the main factor in determining the magnetic properties of UH_3. The large U-U distance in UH_3 as compared with that in uranium metal might be the reason for the partial localization of the $5f$ electrons in UH_3. On the other hand, there is an overlap between the hydrogen-electron states and the $5f$-electron states.

TABLE I. Magnetic properties of β-UH_3.

n_f	n_p	T_C	Θ_C	Reference
0.65	2.44		173	1
0.7, 0.9[a]	2.79	173	137	2
0.6,[a] 1.2[b]		175		3
1.39[c]		175		5
0.7, 0.9[a]		181	173	6
0.7		181	176	7

[a]Magnetization measurements (weak external field).
[b]Magnetization measurements in external field up to 11.5 kOe.
[c]Neutron diffraction.

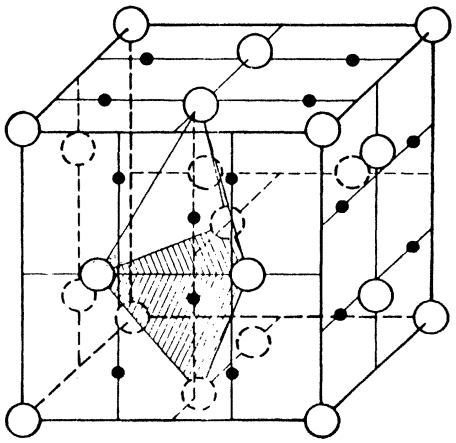

FIG. 1. Crystal structure of β-UH_3. ○, uranium atoms; ●, hydrogen atoms. Not all the hydrogen atoms are shown.

The exact picture is thus rather complicated, as discussed by Switendick.[9]

An interesting approach in attempting to understand the magnetization in β-UH_3 and to bridge the gaps between the different experimental results (Table I) was presented by Agyei.[10] He applied the group-theoretical approach to cell-preserving magnetic transitions. According to his calculations β-UH_3 is not a simple ferromagnet. His proposed magnetic structure is composed of pairs of collinear spins, a part of which are antiparallel, so that the total magnetization per uranium atom is, on the average, only a quarter of that of the single ion for zero external magnetic field $H_0=0$, and half of the value of the single ion when H_0 is applied parallel to one of the $\langle 100 \rangle$ directions of the β-UH_3 crystal. Agyei's calculations do not give the structure for an arbitrary direction of the external field.

Nuclear magnetic resonance (NMR) is an important tool in studying microscopic magnetic properties. The NMR of hydrogen in paramagnetic β-UH_3 was studied by some groups.[4,11,12] As discussed by Grunzweig-Genossar *et al.*[4] an external magnetic field H_0 magnetizes the $5f$ electrons which in turn polarize the s-like conduction electrons through the f-s exchange coupling [the Ruderman-Kittel-Kasuya-Yosida (RKKY) model]. The s electrons have nonvanishing amplitudes at the hydrogen-nuclei sites. The Fermi-contact term gives rise to an internal (hyperfine) magnetic field at the proton site. The NMR frequency of the proton is thus shifted by this "transferred hyperfine" field. The measured parameter of this shift is the paramagnetic shift K_p. By measuring K_p as a function of T and comparing it with the susceptibility χ data at the same temperatures, Grunzweig-Genossar *et al.* were able to plot K_p vs χ, the slope of which yields the transferred hyperfine-field constant $H_{\rm hf}^p$. They found $\partial K_p/\partial\chi=0.4$ mole/emu from which $H_{\rm hf}^p=N_A\mu_B\,\partial K_p/\partial\chi=2.2$ kOe/μ_B, where N_A is Avogadro's number.

In the ferromagnetic phase we expect a similar transferred hyperfine field to be induced on the protons by the spontaneous magnetization. This means that the NMR of protons in ferromagnetic β-UH_3 could give important information on the spontaneous magnetization. To our best knowledge, the NMR of hydrogen in ferromagnetic β-UH_3 has not yet been observed, and here we present the first study of this subject.

II. EXPERIMENTAL SETUP

Uranium wire (nuclear pure) was placed in a quartz tube and hydrogenated in a standard Sievert's apparatus. The hydrogenation was carried out at about 250 °C under ~700-Torr initial hydrogen pressure. The hydrogen gas was taken from an ultrahigh-purity (99.999%) commercial cylinder without further purification. At the end of the hydrogenation process the sample was thermally cycled in the temperature range 250–500 °C in order to assure complete and homogeneous hydrogenation. Then, the hydride was transferred (sealed in the quartz tube under ~400-Torr hydrogen pressure) to a dry-argon-atmosphere glovebox where a thick silicon grease was mixed with the powdered hydride. This was done in order to prevent the free movement of the powder particles. The resulting slurry was sealed in the quartz tube under ~300-Torr helium pressure. Part of the slurry was analyzed by x-ray diffraction which revealed the presence of a pure β-UH_3 phase.

The NMR measurements were carried out with a pulsed NMR system operating in the range of 5–90 MHz with up to 5-kW pulses. In order to find the proton signal at zero external field it was important to first estimate the internal field. An estimate could be made by taking one of the values of n_f given in Table I and assuming that the value of the transferred hyperfine-field constant in the ferromagnetic phase $H_{\rm hf}^f$ is similar to that of $H_{\rm hf}^p$. The internal field is then given by $\vec{\rm H}_{\rm int}=n_f\vec{\rm H}_{\rm hf}^f$, to which the contribution of the dipolar interaction is added to obtain the total effective field $\vec{\rm H}_{\rm eff}$ on the protons. However, this field was measured directly by Gmal *et al.*,[13] who used inelastic neutron scattering to obtain $H_{\rm eff}=4.5\pm0.6$ kOe which corresponds to $\nu_0=19.6\pm2.5$ MHz.

Our first attempts to observe the spin-echo signal were made on β-UH_3 powder in a helium atmosphere. Large acoustic signals were obtained because the particles were free to move. When the powder was mixed with silicone grease these signals decayed permitting the observation of the NMR signal in a very large frequency range, $\nu=14$–25 MHz. The spectrum at 85 K is given in Fig. 2 after normalizing it to the sensitivity factor $\nu^{3/2}$. The center of the line is at 19.4 ± 0.5 MHz, and the linewidth at half-intensity is about 6 MHz. These numbers are very close to the results of Gmal *et al.*[13]

The NMR spectra were also measured in the external magnetic field by sweeping the field at different frequencies. The line for $\nu_0=47.0$ MHz is given in Fig. 3. The peak at 11 kOe is due to protons in the silicone grease. It is broadened by the dipolar fields from the β-UH_3 particles, but as seen from Fig. 3, it stays sharp enough to be

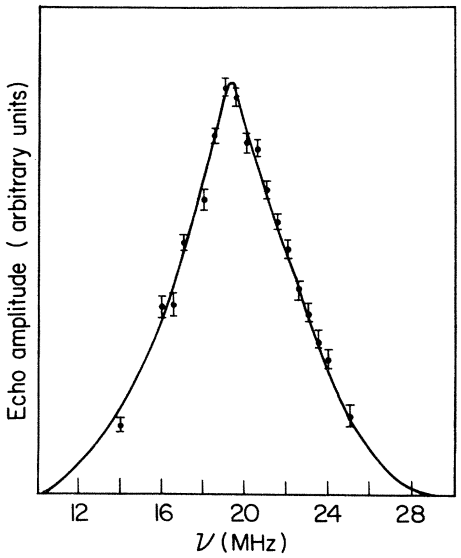

FIG. 2. NMR spectrum of protons in β-UH_3 at $T=85$ K and zero external field after normalization by sensitivity factor of $\nu^{3/2}$. The line is centered at $\nu_0=19.4\pm0.5$ MHz. The linewidth is $\Delta\nu\simeq6$ MHz.

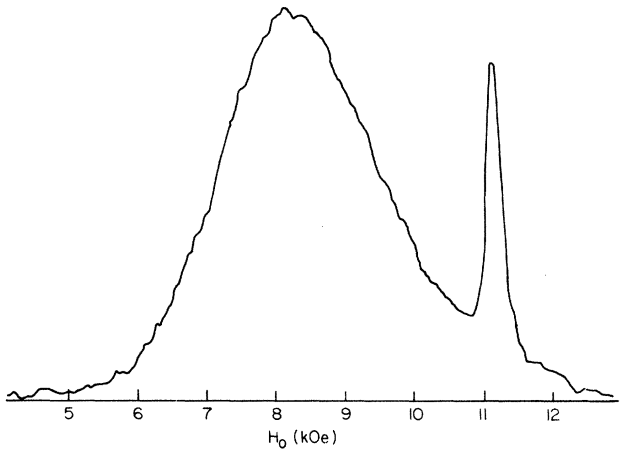

FIG. 3. NMR spectrum of protons in ferromagnetic β-UH_3 measured by sweeping H_0 at $\nu_0=47$ MHz and $T=85$ K. The narrow peak at $H_0=11.04$ kOe is due to protons in silicone grease.

used for calibration of the external field.

The frequency dependence of the central field of the spectrum is given in Fig. 4. It shows a linear behavior for fields large enough to saturate all the particles in the powder, $H_0>4\pi M$, where M is the magnetization per cm^3. The slope of the line corresponds to $\gamma_{expt}/2\pi=4.28\pm0.05$ kHz/Oe, and taking into account the measured linewidth (Fig. 3), it is in good agreement with the value of the proton gyromagnetic ratio $\gamma/2\pi=4.258$ kHz/Oe.

III. NMR SPECTRA

A. Zero-field spectrum

β-UH_3 is a well-defined stoichiometric compound. Its crystallographic structure, as was studied by Rundle,[14] is shown in Fig. 1. The structure is cubic with eight formula units per unit cell. The uranium atoms occupy the two (nonequivalent) sites of β-W ($A15$) lattice,

$$U_I:\ (0,0,0),\ (\tfrac{1}{2},\tfrac{1}{2},\tfrac{1}{2}),$$

$$U_{II}:\ (\tfrac{1}{4},\tfrac{1}{2},0),\ (\tfrac{3}{4},\tfrac{1}{2},0),\ (0,\tfrac{1}{4},\tfrac{1}{2}),$$

$$(0,\tfrac{3}{4},\tfrac{1}{2}),\ (\tfrac{1}{2},0,\tfrac{1}{4}),\ (\tfrac{1}{2},0,\tfrac{3}{4}).$$

The 24 hydrogen atoms are all equivalent. They occupy the tetrahedral sites so that though the tetrahedrons of one U_I and three U_{II} atoms are deformed, the hydrogen atom is at the point which is equidistant to all these uranium atoms,

$$H:\ \pm(0,u,\pm 2u),\ \pm(\tfrac{1}{2},\tfrac{1}{2}\pm 2u,\tfrac{1}{2}+u)$$

cyclic, with $u=\frac{5}{32}$. The lattice constant is $a_0=6.631$ Å.

With the magnetization of the uranium atoms, the hydrogen sites become inequivalent, even in the simple ferromagnetic (or paramagnetic) phase. This is due to the local dipolar field $\vec{H}_d$ which differs from site to site, giving rise to line splitting or line broadening, as was observed. In what follows we will treat this point in more detail.

The NMR frequency of a hydrogen nucleus in ferromagnetic β-UH_3 is given by

$$\nu=\frac{\gamma}{2\pi}\left|\vec{H}_{int}+\vec{H}_d+\vec{H}_L+\vec{H}_D+\vec{H}_0\right|, \tag{1}$$

where the dipolar field due to the local uranium $5f$ electrons is given here by its three parts: $\vec{H}_d$ is the local dipolar field in a Lorentz sphere, $\vec{H}_L=4\pi\vec{M}/3$ is the Lorentz field, and $\vec{H}_D=-D\vec{M}$ is the demagnetization field. For zero external field the sample has ferromagnetic domains so that $\vec{H}_D=\vec{0}$ and Eq. (1) becomes

$$\nu=\frac{\gamma}{2\pi}\left|\vec{H}_{int}+\vec{H}_d+\vec{H}_L\right|. \tag{2}$$

$\vec{H}_d$ is found for each hydrogen site i by a lattice sum over all the uranium magnetic moments $\vec{\mu}_j$ in a sufficiently large sphere around this site,

$$\vec{H}_d^{\,i}=\sum_j\left[\frac{3\vec{r}_{ij}(\vec{\mu}_j\cdot\vec{r}_{ij})}{r_{ij}^5}-\frac{\vec{\mu}_j}{r_{ij}^3}\right]. \tag{3}$$

Here $\vec{r}_{ij}$ is the displacement vector from the hydrogen i to $\vec{\mu}_j$. $\vec{H}_{int}=n_f\vec{H}_{hf}^{\,f}$ and is parallel to $\vec{M}$. The value of H_{hf}^f could be approximated by the value of H_{hf}^p. Measurements of NMR of ^{27}Al in $GdAl_2$ and $DyAl_2$ have shown that the transferred hyperfine-field constants in the ferromagnetic and paramagnetic states are equal.[15] We thus assume that such an equality holds also for β-UH_3 and that (in units of kOe/μ_B)

$$H_{hf}^f=H_{hf}^p=2.2\pm0.16.$$

As was found from neutron diffraction, U_I and U_{II} have the same magnetization, and $|\vec{\mu}_j|=n_f\mu_B$ for all j. n_f is thus left as a parameter to be determined from the experimental results. n_f depends on the temperature and on

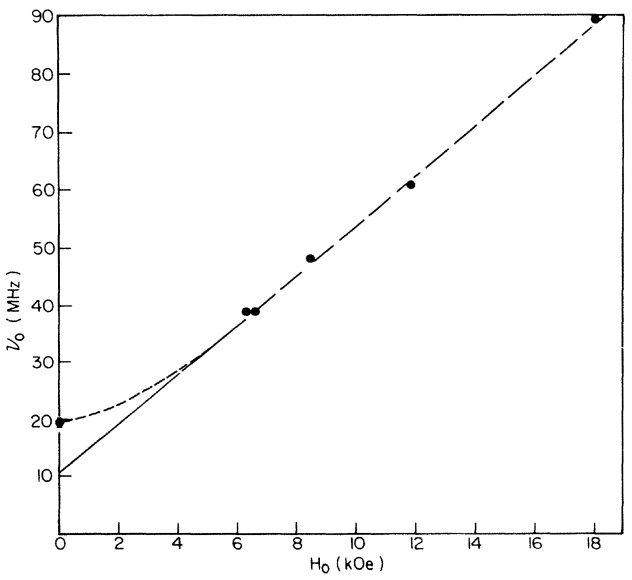

FIG. 4. Dependence of the H_0 of the center of the lines on ν_0. The slope of the line gives $\gamma_{expt}/2\pi=4.28\pm0.05$ kHz/Oe.

H_0.[3,6,7] The magnetization is given by (in units of emu/cm^3)

$$M = 8\mu_B n_f(T,H_0)/a_0^3 = 254 n_f(T,H_0) .$$

For the cubic symmetry of the β-UH_3 lattice the average of H_d^i over all protons is zero (see also next paragraph) and the average resonance frequency ν_0 is given by (in units of MHz)

$$\nu_0 = \frac{\gamma}{2\pi}(H_{\text{int}} + H_L) = \frac{\gamma}{2\pi}(2.2\pm 0.16 + 1.06) n_f(T,0) .$$

From $\nu_0 = 19.4\pm 0.5$ MHz (Fig. 2) we obtain $n_f(85\ \text{K}) = (1.4\pm 0.1)\mu_B$. Taking into account the results of the magnetization measurements[6] which give for $T = 85$ K and $H_0 = 0$, $M = 0.95 M_0$, where M_0 is the spontaneous magnetization at 0 K, we obtain $n_f = (1.46\pm 0.1)\mu_B$.

In a simple ferromagnetic or paramagnet all the magnetic moments are aligned in the direction of the easy axis or the external field. This direction is denoted by a unit vector $\vec{n}$. $\vec{H}_d$ is then given by

$$\vec{H}_d^{\,i} = n_f \overleftrightarrow{D}_i \cdot \vec{n} , \tag{4}$$

where $\overleftrightarrow{D}_i$ is a traceless tensor. For the four hydrogen sites with $x = 0$ (in the unit cell) $\overleftrightarrow{D}_i$ is given by

$$\overleftrightarrow{D}_i = \begin{bmatrix} D_{xx} & 0 & 0 \\ 0 & D_{yy} & \pm D_{yz} \\ 0 & \pm D_{yz} & D_{zz} \end{bmatrix} . \tag{5}$$

Two of these sites are with the $(+)$ sign and two with the $(-)$ sign. Lattice sums with a sufficiently large Lorentz-sphere radius ($R > 10a_0$) for convergence yield $D_{xx} = -567$ Oe (for $1\mu_B$ for μ_j), $D_{yy} = 167$ Oe, $D_{zz} = 400$ Oe, and $D_{yz} = 400$ Oe. The six permutations of coordinates of $\overleftrightarrow{D}_i$ will yield the dipolar tensor for all 24 hydrogen sites in the unit cell. This symmetry of the lattice and the relation,

$$D_{xx} + D_{yy} + D_{zz} = 0 ,$$

causes the average of $\overleftrightarrow{D}$ over all 24 hydrogen sites to be the null tensor for any $\vec{n}$. The lattice sums here are in agreement with those of Grunzweig-Genossar *et al.*[4] They calculated the sums for hydrogen sites which are not exactly at the centers of the uranium tetrahedrons ($u = \frac{5}{32}$), but rather at sites with $u = 0.155$. This accounts for the small difference between their results and ours. Diagonalization of $\overleftrightarrow{D}_i$ gives the following eigenvalues: $\lambda_1 = -567 n_f$ Oe, $\lambda_2 = -133 n_f$ Oe, and $\lambda_3 = 700 n_f$ Oe. The principal axes are found by rotation of the coordinate system at an angle of $+37°$ or $-37°$ in the yz plane.

The easy axis of ferromagnetic β-UH_3 is not known. It is thus interesting to find what kind of spectrum is expected for magnetization in one of the main [100], [110], or [111] crystallographic directions. The calculations were done using Eqs. (2) and (4) for $1\mu_B$ per uranium atom. The results are given in Fig. 5 in the form of stick diagrams. It shows the frequencies of the groups of equivalent protons for each direction with their relative weights, which are summed up to 24, the number of protons in the unit cell.

The experimental spectrum in Fig. 2 shows only a small structure and it is difficult to compare it with any of the stick diagrams of Fig. 5. Thus it would be difficult to derive the easy axis of the magnetization from the spectrum. It is also evident that there is a large broadening of the lines which probably masks a spectrum due to the easy-axis direction of magnetization or a distribution in the directions of magnetization in the sample.

In the usual cases, NMR in ferromagnets benefits from high enhancement of the external rf field, and of the signal, due to high hyperfine fields. Also, in many cases the enhancement in the domain walls is larger than in the domains, and the NMR signals come mainly from the walls which have a distribution of the directions of magnetization. This case is not applicable here due to the small hyperfine field on the protons. Thus almost no enhancement is expected, either in the walls or the domains. It is concluded that the signal comes from the whole sample, that is, both domain and walls.

The cause of the broadening of the spectrum is not clear. It might result from imperfections in the local crystal structure. The transferred hyperfine field is very sensitive to displacements, changes in local density of electronic states, and changes in magnetization. A small amount of oxygen impurities, as well as strain fields or magnetostriction, could cause such changes. The second moment of the experimental line was calculated by numerical integration, and it is given by the square of half of the linewidth at half-intensity $M_2^0 = 5.0\times 10^5$ Oe^2.

B. Spectrum with external magnetic field

When the powder of the ferromagnetic sample is put in an external magnetic field sufficiently large ($H_0 > 4\pi M$) to eliminate all domain walls and to overcome the coercive force ($H_0 > H_c$), all spins in the sample are aligned parallel to H_0, i.e., in a random orientation with respect to the

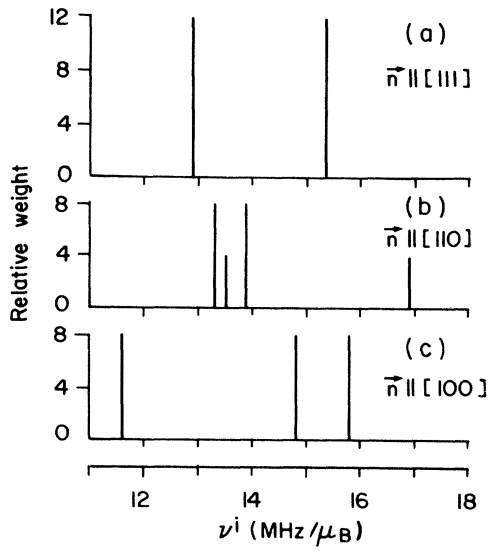

FIG. 5. Stick diagrams of the NMR spectra at $H_0 = 0$ calculated for three possible directions of the easy axis. The frequencies are calculated for $n_f = 1\mu_B$ per uranium ion.

crystallographic axes. For β-UH_3 with $H_c \simeq 4$ kOe at 85 K (Ref. 6) and $4\pi M \leq 4.5$ kOe (for $n_f \leq 1.4$ from Table I) this alignment will take place if $H_0 > 4.5$ kOe. Further increase in H_0 above this value will change the frequency directly by $\gamma H_0/2\pi$, as shown in Fig. 4. The small increase of M with H_0 above 7 kOe (Ref. 6) might be the reason for the experimental γ_{expt} to be slightly larger than the γ of protons.

The case of NMR in ferromagnetic particles magnetized by H_0 is very similar to that in magnetized paramagnetic powder[4] especially close to Θ_C and with high H_0. It is thus interesting to compare the line shapes in both phases. We have calculated the absorption line of β-UH_3 at 202 K and $H_0' = 3.74$ kOe by integrating the derivative spectrum shown in Fig. 6 of Ref. 4. This calculated line is given in Fig. 6. Its linewidth at half-intensity is $\Delta H^p = 38$ $\pm 3\%$ Oe. This line was compared with the absorption spectrum measured at 85 K and $\nu_0 = 60.9$ MHz. Good agreement in shape was found, indicating that the broadening comes from the same mechanism. It is to be noted that for both spectra motional narrowing is neglected,[4,12] and the dipolar proton-proton interaction has a small second moment $M_2 = 23.0$ Oe^2,[4] which hardly changes the spectrum. ΔH^p is scaled to $M = \chi H_0'$ as is the width in the ferromagnetic phase, $\Delta H^f = 2.83(\pm 3\%)$ kOe to M^f. Taking $\chi = 1.4 \times 10^{-3}$ ($\pm 8\%$) emu/cm^3 as an average value of the published results,[1,2,6,7] we find (in units of emu/cm^3)

$$M^f = \chi H_0' \, \Delta H^f / \Delta H^p = 390 \ (\pm 10\%) \ .$$

Taking into account that[6] $M^f = 1.06 M_0$ (at $T = 85$ K and $H_0 = 12$ kOe) and, with the spontaneous magnetization, $M_0 = 254 n_f$ Oe, we find $n_f = 1.45$ ($\pm 10\%$), which is in good agreement with the zero-external-field results.

The shape of the NMR line is not symmetric. This is due to a distribution in the effective fields on the protons. In addition to the distribution in $\vec{H}_{\text{int}}$, which was discussed for the line measured at $H_0 = 0$, there is the distribution in $\vec{H}_d$ that for this case is different than for $H_0 = 0$. To these two is added the distribution in $\vec{H}_D$, which is due to the distribution in particle shapes. The line shape due to the distribution in $\vec{H}_d$ was studied by Bloembergen and Rowland,[16] and Kroon.[17] The tensor $\overleftrightarrow{D}_i$ in Eq. (4) is diagonalized with $\lambda_1 \leq \lambda_2 \leq \lambda_3$. In terms of the parameters $\Delta_{ij} \equiv \lambda_i - \lambda_j$ and $Q_r \equiv \Delta_{32}/\Delta_{21}$, the distribution function is given by[17]

$$f_d(H_d) = \begin{cases} [(\lambda_3 - H_d)\Delta_{21}]^{-1/2} K[Q_r(H_d - \lambda_1)/(\lambda_3 - H_d)] \ , & \lambda_1 \leq H_d \leq \lambda_2 \\ [(H_3 - \lambda_1)\Delta_{32}]^{-1/2} K\{(\lambda_3 - H_d)/[(H_d - \lambda_1)Q_r]\} \ , & \lambda_2 \leq H_d \leq \lambda_3 \\ 0, \ H_d < \lambda_1, \ H_d > \lambda_3 \end{cases} \tag{6}$$

where

$$K(m) \equiv \int_0^{\pi/2} \frac{d\alpha}{(1 - m \sin^2\alpha)^{1/2}} \ . \tag{7}$$

A line is symmetric if $Q_r = 1$. For our values of λ_i found in Sec. III A, $Q_r = 1.92$. Figure 7 shows the resulting line shape as a function of H_0 (rather than H_d) calculated using Eqs. (1) and (6). The asymmetry of the shape is opposite to that of the experimental line (Fig. 6). Only $Q_r < 1$ would give an asymmetry in the appropriate direction. Owing to the large overlap of the $5f$ electrons of the first uranium neighbor and the hydrogen site,[9] the dipoles of these first neighbors might not be considered fully local for dipolar field calculations. The sum over all the uranium ions except the first neighbors gives $Q_r = 0.004$. Thus if the contribution of the first neighbors is much smaller than $n_f \mu_B$, then $Q_r < 1$.

The second moment of the distribution in H_d is given by[4]

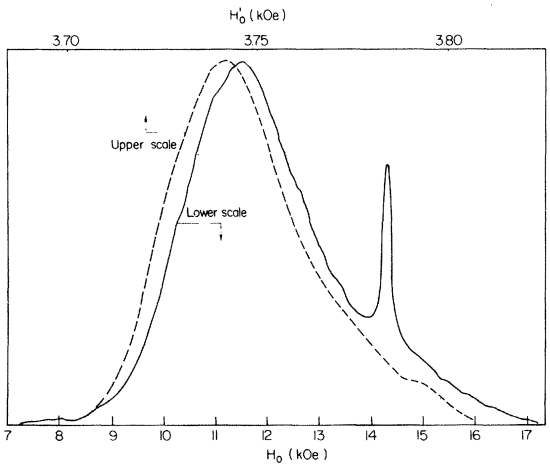

FIG. 6. Comparison between the shapes of NMR spectra of protons measured in ferromagnetic β-UH_3 (solid curve) and in paramagnetic β-UH_3 (dashed curve). The spectrum in the ferromagnetic phase was measured at $T = 85$ K and $\nu_0 = 60.9$ MHz; external field is given by the lower scale (H_0). The spectrum in the paramagnetic phase was obtained by numerical integration of the derivative curve measured by Grunzweig-Genossar *et al.* (Ref. 4) at 202 K and 16 MHz; external field is given by the upper scale (H_0').

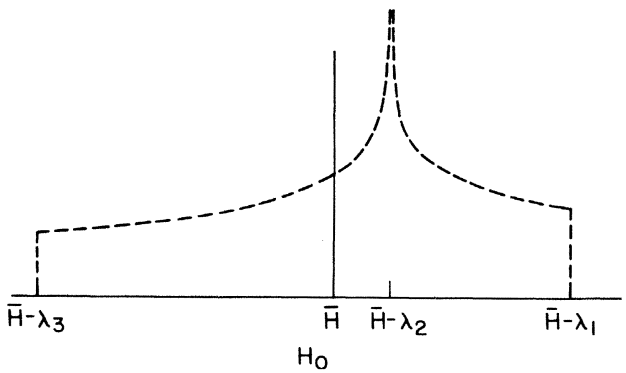

FIG. 7. Line shape due to distribution of $\vec{H}_d$ as calculated from Eqs. (1) and (6) ($\overline{H} = 2\pi\nu/\gamma - |\vec{H}_{\text{int}} + \vec{H}_L + \vec{H}_d|$).

$$M_2^d=\tfrac{2}{15}(\lambda_1^2+\lambda_2^2+\lambda_3^2)\ . \tag{8}$$

For $M^f=390$ emu, the lattice sums give $\lambda_1=-870$ Oe, $\lambda_2=-205$ Oe, $\lambda_3=1075$ Oe, and $M_2^d=2.61\times10^5$ Oe^2. The second moment of the experimental line (Fig. 6) is (in units of Oe^2)

$$M_2^{(\text{expt})}\simeq(\Delta H^f/2)^2=2.0\times10^6\ ,$$

which shows that H_d is too small to account for the linewidth. A smaller contribution of the first uranium neighbors will make M_2^d even less important. Thus the distribution in $\vec{H}_d$ could not be responsible for the measured line shape.

The demagnetization fields, when originated from shapes of particles randomly distributed around a sphere, give rise to a Gaussian line shape[18] centered at $H_0=-4\pi M/3$ with a linewidth of $4\pi M/3$, so that (in units of Oe^2)

$$M_2^D\simeq\left[\frac{2\pi M^f}{3}\right]^2=6.7\times10^5\ .$$

The experimental line shape with a tail towards higher fields shows that the particles have, on the average, a contracted form. We take a spheroid of revolution with certain dimensions as the average form of the particles. The demagnetization fields of such a spheroid are given by

$$H_D=-\frac{4\pi M}{3}-2\pi M\eta(3\cos^2\theta-1)\ , \tag{9}$$

where $-\frac{1}{3}\le\eta\le\frac{2}{3}$ shows the derivation from a sphere. $\eta>0$ for a contracted spheroid and $\eta<0$ for an extracted spheroid. Equation (9) yields a distribution of the effective field which is similar to that in a powder sample due to an axial anisotropy field. The second moment of this distribution is given by[4]

$$M_2^\eta=\tfrac{1}{5}(4\pi M\eta)^2\ . \tag{10}$$

From $M_2^{\text{expt}}=M_2^0+M_2^d+M_2^D+M_2^\eta$, we find $M_2^\eta=5.7\times10^5$ Oe^2. This gives $\eta=+0.34$, which corresponds to a ratio of 0.29 between the polar and azimuthal axes.[4]

C. Spectrum calculated for Agyei's model

The structure proposed by Agyei[10] for ferromagnetic β-UH_3 at $H_0=0$ is given in Fig. 8. We have calculated the NMR spectrum for this structure. We assume that H_{hf} comes from interactions with the four first neighbors only. For the hyperfine interaction

$$\mathscr{H}_{\text{hf}}=\sum_{j=1}^{4}A_j\vec{I}\cdot\vec{J}_j\ ,$$

we assume that all four hyperfine constants A_j are equal, and thus the hyperfine field arising from each neighbor is a quarter of the total hyperfine field, namely $H_{\text{hf}}/4$. Denoting the direction vector of $\vec{J}_j$ by $\vec{n}_j$ the internal field on the proton is given by

$$\vec{H}_{\text{int}}=\tfrac{1}{4}H_{\text{hf}}n_f\sum_{j=1}^{4}\vec{n}_j\ . \tag{11}$$

Following Eq. (2) we calculate ν by adding $\vec{H}_d$, calculated for Agyei's model, and $\vec{H}_L$, calculated for $\frac{1}{4}n_f\mu_B$ for each uranium. For $\frac{1}{4}n_f$ we take the smaller measured value of n_f from Table I (that of Henry[3]), $\frac{1}{4}n_f=0.6$. The calculated spectrum is given in the form of a stick diagram in Fig. 9(a). It is evident that there is no agreement between this spectrum and the experimental results (Fig. 2). Even if line broadening eliminates the structure of the spectrum and n_f is changed, the spectrum is still much larger than the experimental line. In order to verify the experimental spectrum we have looked for NMR absorption up to 42 MHz, but could not find additional lines similar to those of Fig. 2.

The alternative structure proposed by Agyei[10] is derived from that of Fig. 8 by reversing the directions of moments localized at the $(\frac{1}{2},0,\frac{3}{4})$ and $(\frac{1}{2},\frac{1}{2},\frac{1}{2})$ sites. The calculated spectrum for this structure is given by Fig. 9(b). It is clear that this magnetic structure is also not in accord with the experimental results.

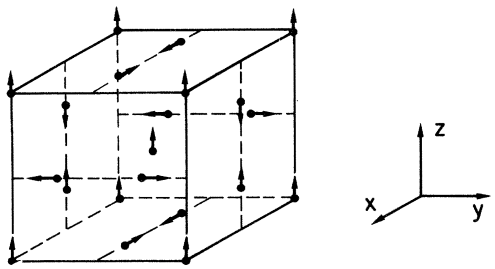

FIG. 8. Structure of magnetically ordered β-UH_3 in zero external magnetic field, as presented by A. K. Agyei (Ref. 10). The structure obtained by reversing the directions of moments localized at the $(\frac{1}{2},0,\frac{3}{4})$ and $(\frac{1}{2},\frac{1}{2},\frac{1}{2})$ sites is also admissible (Ref. 10).

IV. TRANSVERSE RELAXATION

The transverse relaxation for $H_0=0$ was measured at two temperatures, $T=4.2$ and 85 K. The relaxation was found to be exponential with relaxation times $T_2=90\pm5$ μsec (4.2 K) and $T_2=40\pm5$ μsec (85 K). T_2 becomes longer when an external field is applied, as shown in Fig. 10.

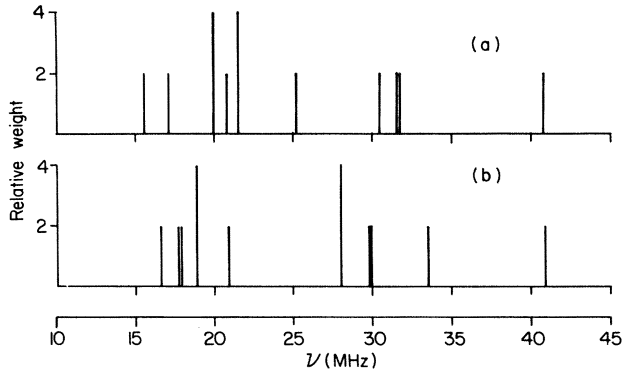

FIG. 9. Stick diagram of NMR spectra calculated: (a) for the magnetic structure of Fig. 8, and (b) for the magnetic structure which is obtained from Fig. 8 by reversing the directions of the moments at the $(\frac{1}{2},0,\frac{3}{4})$ and $(\frac{1}{2},\frac{1}{2},\frac{1}{2})$ sites.

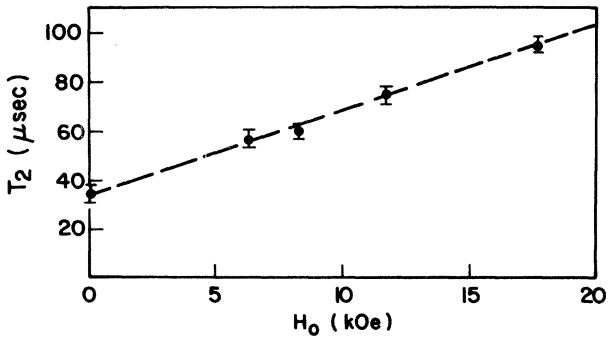

FIG. 10. Transverse relaxation time T_2 at 85 K and different external magnetic fields.

An interaction which was previously found to give rise to field-dependent transverse relaxation[18] is the Suhl-Nakamura (SN) interaction. However, it goes through the hyperfine interaction, which is weak in β-UH_3. Thus the influence of the SN interaction in β-UH_3 is expected to be small. The second moment for SN interaction is given by[19]

$$M_2^{\mathrm{SN}}=\frac{I(I+1)}{24\pi S^2}\frac{\omega_n^4}{\omega_{\mathrm{ex}}^{3/2}\omega_{\mathrm{an}}^{1/2}}, \tag{12}$$

where $\omega_n\equiv 2\pi\nu_0$, $\hbar\omega_{\mathrm{ex}}\sim k_B T_c$, and $\hbar\omega_{\mathrm{an}}\equiv 2\mu_B\times(H_{\mathrm{an}}+H_0)$, where H_{an} is the anisotropy field. For $H_0=0$, ω_{an} was found from $\hbar\omega_{\mathrm{an}}=K$, where the anisotropy constant $K=8\times 10^{-17}$ erg.[6] The relaxation time was estimated by $T_2^{\mathrm{SN}}=(M_2^{\mathrm{SN}})^{-1/2}\simeq 14$ msec for the zero-external-field experiment.

The second moment of the hydrogen nuclear-dipole—nuclear-dipole interaction is given by[20]

$$M_2=\tfrac{3}{5}\gamma^4\hbar^2 I(I+1)\sum_j r_{ij}^{-6}, \tag{13}$$

where r_{ij} is the distance between hydrogen i and hydrogen j. This gives $T_2=(M_2)^{-1/2}\simeq 8$ μsec. The longer and exponential relaxation obtained experimentally indicates a mechanism of narrowing due to microscopic inhomogeneous broadening.[21] As discussed above, the dipolar fields of the different sites in the unit cell, $\vec{H}_d^{\,i}$ of Eq. (3), are different from site to site, both in value and in direction. The interaction between neighboring spins with different energies is less effective due to energy conservation.[21] This "dilution" is further enhanced by the need for angular momentum conservation which strongly decreases the efficiency of the interaction between noncollinear spins. Only terms with operators such as $I_i^+ I_j^z$ might give rise to mutual spin flips of such spins. This effect of "energy dilution" and "angular dilution" divides the nuclear spins into 12 groups, each group with two protons per unit cell. The protons in each group are equivalent, i.e., $\vec{H}_{\mathrm{eff}}^{\,i}=\vec{H}_{\mathrm{eff}}^{\,j}$ for each two protons i and j within the group. For a general direction of $\vec{n}$ the 12 groups are all inequivalent and the spin-spin interaction is effective only between protons of the same group. For $\vec{n}\|[100]$ the protons might have one out of three energies, as shown in Fig. 5. The angular dilution, however, further divides them into one group with eight protons per unit cell and eight groups with two protons per unit cell. For $\vec{n}\|[110]$ the four groups of protons with different energies are divided by the angular dilution into twelve two-proton groups of equivalent sites (as in the case of a general direction of $\vec{n}$). For $\vec{n}\|[111]$ there are two groups of protons with different energies divided into twelve groups of equivalent sites.

For each group of equivalent protons T_2 was calculated separately by[20]

$$M_2=\tfrac{3}{4}I(I+1)\gamma^4\hbar^2\sum_j(3\cos^2\theta_{ij}-1)r_{ij}^{-6}, \tag{14}$$

where θ_{ij} is the angle between $\vec{r}_{ij}$ and $\vec{n}$. For $\vec{n}\|[100]$ we found, for $T_2=(M_2)^{-1/2}$, the following values: $T_2(1)=11$ μsec, $T_2(2)=59$ μsec, and $T_2(3)=95$ μsec, corresponding to the three groups of protons with different energies, each group with the weight $A_i=8$ for $i=1,2,3$ (see Fig. 5). In the case of $\vec{n}\|[110]$ we obtained $T_2(i)=148$, 47, 106, and 29 μsec, corresponding to the four energies with the weights $A_i=8,4,8,4$. For $\vec{n}\|[111]$, $T_2(1)=55$ μsec and $T_2(2)=55$ μsec, and $A_i=12$ for $i=1$ and 2.

The ratio of the fourth moment (also calculated) and the square of the second moment for each group was close to 3, which means that the transverse relaxation of each group is Gaussian. Owing to the line broadening the NMR signal comes from some (or all) of the groups, and the decay is given by

$$F(t)=\sum_{i=1}^{m}A_i\exp\left[\frac{-t^2}{2[T_2(i)]^2}\right], \tag{15}$$

where m is the number of groups of protons with different energies. $F(t)$ was calculated for the three directions of $\vec{n}$ and compared with the experimental relaxation at $T=4.2$ K and $H_0=0$. Good agreement was found with $F(t)$ of $\vec{n}\|[110]$, as shown in Fig. 11. This good agreement indicates that the mechanism discussed above might explain the transverse relaxation. This model, however, is too crude for determining the direction of the easy axis.

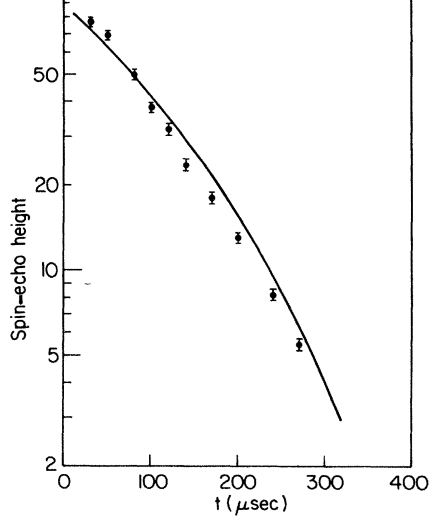

FIG. 11. Transverse relaxation of the spin echo of protons in ferromagnetic β-UH_3 measured at $T=4.2$ K. The solid line is calculated using Eq. (15).

The weak dependence of T_2 upon temperature, changing from $T_2=90$ μsec at 4.2 K to 40 μsec at 85 K, is difficult to explain. It is possible that interactions through the conduction electrons, such as RKKY, become effective as the temperature rises, due to the excitation of electrons with energies close to the Fermi level. T_2 becomes longer when an external field is applied (Fig. 10). This indicates that the external field dilutes the equivalent protons. The magnetostriction might be the mechanism by which the crystal is deformed and equivalent protons become inequivalent.

V. DISCUSSION

The NMR results yield a value of $n_f=1.45\pm0.1\mu_B$ per uranium atom in β-UH_3 at 0 K. This value is in good agreement with the neutron-diffraction results given in Table I,[5] where the value $n_f=1.38\mu_B$ was found. Neutron diffraction, as well as NMR, measures the microscopic properties of the substance. The other results in Table I were found by macroscopic measurements of the magnetization while applying an external magnetic field. In such measurements the external field first overcomes the coercive force and eliminates the domain walls. Then it has to overcome the crystal field in order to rotate the spins in the domains to the direction of the external field. It is very complicated to extract the magnetization at $H_0=0$ from these measurements in powder samples, when the crystal-field parameters are not known and the nature of magnetization (local or itinerant) is not well understood.

When we were looking for the NMR signal in ferromagnetic β-UH_3, we calculated the frequency by assuming that the hyperfine-field constant in the ferromagnetic state $H_{\rm hf}^f$ is equal to that in the paramagnetic state $H_{\rm hf}^p$. The good agreement of the value of n_f found by NMR with that found by neutron diffraction justifies this assumption. The equality $H_{\rm hf}^f=H_{\rm hf}^p$ is very interesting by itself. Similar results were found for entirely different cases: ^{59}Co in cobalt and ^{61}Ni in nickel, both $3d$ ferromagnetic metals,[22] and ^{27}Al in $DyAl_2$ and $GdAl_2$ with localized $4f$ electrons.[15] The hyperfine constants hardly changed in these metals in a large range of temperatures including the ferromagnetic to paramagnetic phase transition, which is expected to be accompanied by changes in the band structure and thus influences the hyperfine fields. The case of β-UH_3 is exceptional due to the hydrogen atoms involved. First, the contribution of the electrons of these hydrogens to the metallic state is not clear, and second, there is no core polarization and the protons are directly exposed to the influence of the conduction electrons.

The interactions giving rise to the exchange and hyperfine couplings in β-UH_3 were discussed by Grunzweig-Genossar *et al.*,[4] who analyzed the role that the RKKY interaction plays in determining the magnetic properties of this material. However, the lack of sufficient data, such as the exact band structure and the crystal-field parameters, prevents a detailed analysis of the experimental results.

VI. SUMMARY

The observation of the NMR of protons in the ferromagnetic phase of β-UH_3 enables us to study the magnetic properties of this interesting material. The basic parameter, the magnetization per uranium ion, was studied by comparing the spectrum in the ferromagnetic state with previous NMR studies in the paramagnetic state. The magnetization, found from the resonance frequency as well as from the linewidth, is 1.45 ($\pm10\%$) Bohr magneton per uranium, in good agreement with neutron-diffraction results.

The asymmetry of the line shape, measured at $T=85$ K by sweeping the external magnetic field, was the same for that measured in paramagnetic β-UH_3 at $T=202$ K. This shows that the main origin of the inhomogeneous broadening of the spectrum is the same in both cases. The broadening was shown to come from the distribution of the demagnetization fields due to the distribution of the powder-particle forms around the contracted ellipsoid form.

The classical dipolar field arising from the local magnetic moments of uranium atoms is different for different proton sites. This gives rise to the energy and angular dilutions of the proton spins. Second moments of the dipole-dipole internuclear interaction, calculated including like spins only, could explain the measured values of transverse relaxation time T_2. We could only give a qualitative explanation of the behavior of T_2 as a function of the temperature and external magnetic field.

ACKNOWLEDGMENTS

We are grateful to D. Hirshler and Dr. J. Naveh for their help in sample preparation and to Dr. D. Zamir and Dr. G. Cinader for fruitful discussions. This research was supported in part by a grant from the U. S.—Israel Binational Science Foundation, Jerusalem, Israel.

[1]W. Trzebiatowski, A. Sliwa, and B. Stalinski, Rocz. Chem. 26, 110 (1952); 28, 12 (1954).
[2]D. M. Gruen, J. Chem. Phys. 23, 1708 (1955).
[3]W. E. Henry, Phys. Rev. 109, 1976 (1958).
[4]J. Grunzweig-Genossar, M. Kuznietz, and B. Meerovici, Phys. Rev. B 1, 1958 (1970).
[5]C. G. Shull and M. K. Wilkinson, Oak Ridge National Laboratory Report No. ORNL-1879, p. 24 (unpublished), as quoted in Ref. 4. Also, Ref. 4 quotes an unpublished neutron-diffraction study of β-UH_3 by G. P. Felcher, F. A. Smith, and M. Kuznietz, which confirms the results of Shull and Wilkinson.
[6]S. T. Lin and A. R. Kaufman, Phys. Rev. 102, 640 (1956).
[7]A. I. Karchevskii and E. M. Buryak, Zh. Eksp. Teor. Fiz. 42, 375 (1962) [Sov. Phys.—JETP 15, 260 (1962)].
[8]D. D. Koelling and A. J. Freeman, Phys. Rev. B 7, 4454 (1973).
[9]A. C. Switendick, J. Less-Common Met. 88, 257 (1982).
[10]A. K. Agyei, J. Phys. C 14, 3433 (1981).
[11]W. Spalthoff, Z. Phys. Chem. (Frankfurt am Main) 29, 258 (1961).

[12]G. Cinader, M. Peretz, D. Zamir, and Z. Hadari, Phys. Rev. B 8, 4063 (1973).
[13]B. Gmal, A. Heidemann, and A. Steyerl, Phys. Lett. 60A, 471 (1977).
[14]R. E. Rundle, J. Am. Chem. Soc. 69, 1719 (1947); 73, 4172 (1951).
[15]Y. B. Barash, J. Barak, and N. Kaplan, Phys. Rev. B 25, 6616 (1982).
[16]N. Bloembergen and T. J. Rowland, Acta Metall. 1, 731 (1953).
[17]D. J. Kroon, Philips Res. Rep. 15, 501 (1960).
[18]J. Barak, I. Siegelstein, A. Gabai, and N. Kaplan, Phys. Rev. B 8, 5282 (1973).
[19]H. Suhl, Phys. Rev. 109, 606 (1958).
[20]A. Abragam, *The Principles of Nuclear Magnetism* (Oxford University Press, London, 1961), Chap. IV.
[21]D. Hone, V. Jaccarino, T. Ngwe, and P. Pincus, Phys. Rev. 186, 291 (1969).
[22]M. Shaham, J. Barak, U. El-Hanany, and W. W. Warren, Jr., Phys. Rev. B 22, 5400 (1980).